Journal of
Computational and Theoretical Nanoscience
Vol. 7, 1–10, 2010

Solitonic Ionic Currents Along Microtubules

M. V. Satarić, D. Sekulić*, and M. Živanov

Faculty of Technical Sciences, University of Novi Sad, Trg D. Obradovića 6, 21000 Novi Sad, Serbia

Microtubules are very important cytoskeletal structures implicated in different cellular activities. We should mention the cell division and traffic of organelles (mitochondria, vesicles and other cargos) by kinesin and dynein motor proteins. Microtubules are also playing important roles in higher neuronal functions including mechanisms of consciousness and memory. We here investigate the circumstances and the conditions enabling microtubules to act as nonlinear electrical transmission lines for ions flow along their cylinders. We established a model in which each tubulin dimmer protein is an electric element with a capacitive, resistive and negative incrementally resistive property due to polyelectrolyte nature of microtubules in cytosol. The particular attention was paid to the role of nano-pores existing between neighboring dimmers within a MT wall which exhibit properties like ionic channels. These nano-pores are candidates to explain some properties of microtubules resembling to unipolar transistors enabling the rectification and amplification of ionic currents.

Keywords: Cytoskeleton, Microtubule, Polyelectrolyte, Nonlinear Transmission Line, Ionic Waves, Soliton, Nano-Pore.

1. INTRODUCTION

The cytoskeleton consists of three mayor types of thin rod-like filaments that span the cytoplasm: actin-based filaments (i.e., microfilaments), tubulin-based filaments (i.e., microtubules-MTs) and intermediate filaments (e.g., neurofilaments-keratin). There are at list three well-studied mechanical functions of the cytoskeleton *in vivo*, providing the mechanical strength of the cell, segregating the chromosomes and participating in the cellular traffic.[1]

MTs are long and rigid tubulin polymers. They are the key protein filaments that form several μm long hollow cylinders typically $d = 25$ nm in outer diameter, Figure 1, and exhibit dynamically unstable polymerization kinetics.

MTs are formed as ferroelectric polymers whose building block is a protein called tubulin. The hollow cylindrical wall of a MT is made up of parallel chains or protofilaments of tubulin-hetero-dimer. Each dimer, 8 nm in length, is composed of two units, a α-tubulin and a β-tubulin monomer. Each MT is generally made up of 13 protofilaments *in vivo*. Every tubulin monomer of the MT cylinder has a C-terminal helix, H12, followed by a highly acidic amino-acid sequence protruding out of the MT outer surface and called C-terminus tail (TT). The TTs sequences have length $l_{TT} = 4{,}5$ nm when completely outstretched. The TTs are being essential for MT interactions whit MT associated proteins and motor proteins, (kinesin and dynein).[2,3] More details about TTs structures and properties can be found in Ref. [4]. The shape of tubulin dimer with pertaining TTs is presented in Figure 2, including the detailed charge distributions on the tubulin surface calculated by team lead by Tuszynski.[5]

At neutral pH the negative charge on TT causes it to remain extended due to electrostatic repulsion. Under more acidic conditions the negative charges of pertaining amino acids within TT are partially neutralized by counter-ions condensed on them. This effect allows the β-TTs to be compacted by folding, as shown in Figure 3.

This is the largest structural effect in MTs and this fact has the great importance in establishing of our model with respect to the variable effective electrical capacitance of MTs. The detailed charge distribution on the MT surface, calculated in Ref. [5], enabled the determination of an electrostatic potential around a MT. It exhibits non-uniformity along the MT radius with a peak and a trough corresponding to every of 13 protofilaments and the area between them populated with mentioned nano-pores. These findings play an essential role in presented modeling of MT as a "coaxial cable" for intracellular communication.

In as much MTs are mostly negatively charged on their outer surface they are true polyelectrolyte polymers. This is the consequence of the fact that numerous amino acids forming tubulin have many negatively charged residues under physiological conditions, as was already stressed for TTs. Thus the conditions for application of Manning's theory[6] are provided enabling "condensation" of positive

*Author to whom correspondence should be addressed.

RESEARCH ARTICLE

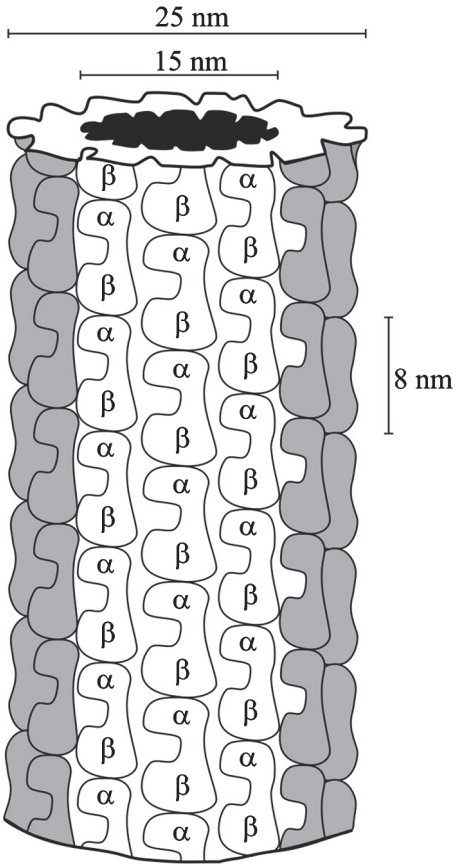

Fig. 1. A MT hollow cylinder of 13 parallel protofilaments with denoted characteristic dimensions: outer and inner diameters of 25 nm and 15 nm and tubulin dimer length of 8 nm.

counter-ions near the negative surface of MT landscape. As a result, every MT attracts positive counter-ions in narrow shell (ionic cloud-IC) near its surface, while negative ions of the cytosol are being repelled such that a roughly

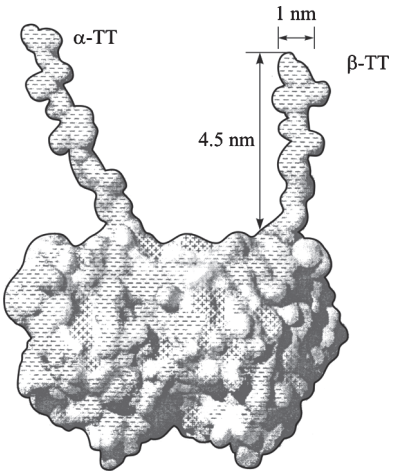

Fig. 2. The landscape of a tubulin dimer with dimensions of TTs the length of 4.5 nm and diameter of 1 nm, and surface charge distribution according to Tuszynski et al.[5]

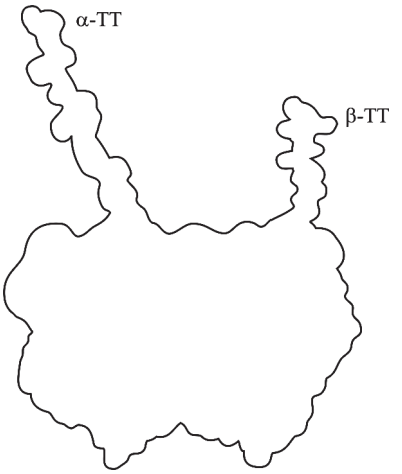

Fig. 3. The shape of TTs, where β-TT is being shrank, thus diminishing its capacity.

cylindrical depletion area around a MT is being created, Figure 4. The thickness of this depleted area is defined by so-called Bjerrum length, which is the distance from the MT surrounding IC at which the Coulomb energy of the screened surface charges equals the thermal energy

$$\frac{e^2}{4\pi\varepsilon_o\varepsilon l_B} = k_B T \tag{1}$$

Here e is the charge of an electron, ε_0 the permittivity of vacuum, ε the relative permittivity of cytosol and k_B is Boltzmann's constant. At a physiological temperature of $T = 310$ K, and taking $\varepsilon = 80$, it is clear from Eq. (1) that we have

$$l_B = 6.7 \times 10^{-10} \text{ m} \tag{2}$$

On the other hand, the thickness of the IC of positive counter-ions is dictated by the surface landscape and by its negative charge distributions. In the case of actin filament, Pollard and Cooper[6] estimated that the radius of IC is of the order of 8 nm, while the filament radius is 2.5 nm, giving IC thickness of 5.5 nm. From the best of our knowledge the evidences for MTs IC thickness are still missing but we anticipate that the corresponding value should be of the order of 2 nm since the surface of MTs is pretty less negative than in actin filament. Significant ionic movements within this bound IC are therefore allowed along the length of the MT provided that it is shielded from the bulk solution by the depletion layer of thickness l_B.

Bearing in mind the IC geometry around the MT we see that effectively MTs may act as biological "electrical wires" which can be modeled as nonlinear inhomogeneous transmission lines that are able to propagate nonlinear dispersive ionic waves. First attempts to elaborate the cytoskeleton as a network of nonlinear polyelectrolyte transmission lines are made by Tusyznski et al.,[7] for actin filaments, and later further elaborated by Sataric et al.[8] Similar approach was applied for MTs in Ref. [4]. Here

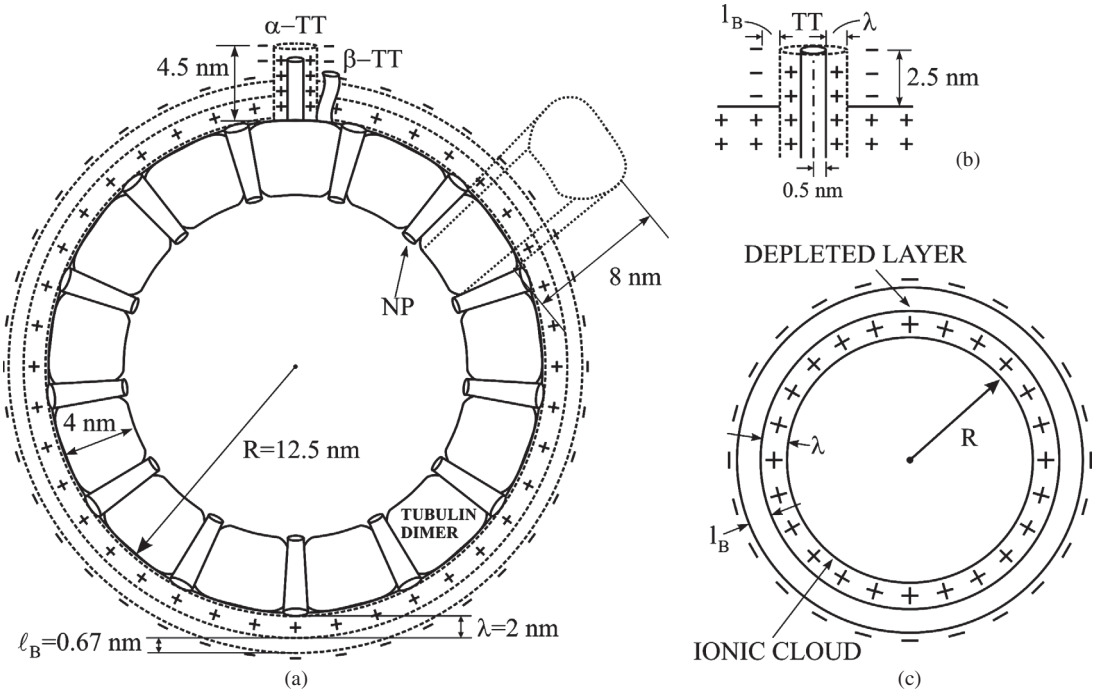

Fig. 4. The geometry of a MT with ionic cloud and depleted layer clearly depicted, including corresponding dimensions: the thickness of IC $\lambda = 2$ nm and Bjerrum length $l_B = 0.67$ nm. The top part of (a) shows α and β TTs.

we further amend the model introduced in Ref. [4] paying particular attention on the role of nano-pores (NPs) embedded in MT wall. In that respect we partially relied on the results published by the group lead by Eisenberg,[9, 10] which emphasize the particular role of calcium ions in dynamics of NPs.

Some fifteen years ago, Lin and Cantiello[11] performed an assay demonstrating that IC waves along a single actin filament were highly nonlinear in nature exhibiting the wave patterns remarkably similar to recorded solitary waveforms from various experimental studies on electrically stimulated nonlinear transmission lines.[12] Recently Tuszynski and Cantiello[13] conducted similar experiment on single MT which even manifested transistor-like amplification of electrical signals. It is our objective in this article to amend our earlier model[3, 4] in order to explain these features of MTs and their possible role in information processing within neurons.

The paper is organized in the following way:

In the Section 2 we reexamined the estimations of elementary capacitance, inductance and resistance components of elementary MT ring and elaborated the role NPs.

The Section 3 is dedicated to the modeling of each MT as a nonlinear C–R–G transmission line and evaluating KdV- like equation and its solution.

Section 4 deals with the influence of viscous dissipation and intrinsic electrical field on the dynamics of ionic solitons along MTs.

The Last section offers the conclusions regarding this interesting physical mechanism in terms of the cell's electrical activity provided by the MTs and their interactions with ions from MT lumen.

2. THE ELEMENTS OF A MT AS AN ELECTRIC TRANSMISSION LINE

The basic assumption is that a MT with condensed counter-ions is separated from the rest of the ions in the bulk solution by a depleted layer which plays the role of a dielectric medium located between MTs and the cytosol solution. This IC is electro-conductive medium responsible for electrical properties of MT. The depleted layer provides that IC and repelled ions represent the "conductive plates" of cylindric capacitor. The ions injected from appropriate cell's compartment are confined to flow parallel with MTs within the IC of the supposed thickness $\lambda = 2$ nm. We here pay particular attention to the case where calcium ions are injected within IC.

2.1. The Capacitance of a MT Elementary Ring

The elementary ring (ER) consists of 13 dimers, Figure 4(a), forming the ring of radius of 12.5 nm and of length $l = 8$ nm. On the basis of the Poisson-Boltzmann equation the detailed derivation given in Ref. [4] yielding the basic capacity of such cylindric ER as follows

$$C_0 = \frac{2\pi\varepsilon_0\varepsilon l}{\ln(1 + (l_B/R))} \tag{3}$$

RESEARCH ARTICLE

where $l = 8 \times 10^{-9}$ m is length of an ER, (length of one tubulin dimer), $\varepsilon_0 = 8.85 \times 10^{-12}$ F/m, $\varepsilon = 80$, $l_B = 0.67 \times 10^{-9}$ m. In contrast to,[4] we here take $R = (d/2 + \lambda) = (12.5 + 2)$ nm leading to elementary capacity:

$$C_0^{(1)} = \frac{6.8 \times 8.85 \times 10^{-12} \times 80 \times 8 \times 10^{-9}}{\ln(1 + (0.67/14.5))} = 0.8 \times 10^{-15} \text{ F} \tag{4}$$

In the same way, we consider an extended TT as a smaller cylinder with the length $l_{TT} = 4.5$ nm and the radius $R_{TT} = 0.5$ nm giving $R = R_{TT} + \lambda = 2.5$ nm. From formula (3) we calculate an additional capacity $C_0^{(2)}$ for $n = 13 \times 2 = 26$ TTs, contained in the same ER, composed of 13 dimers, see Figure 4(a), top position, and Figure 4(b).

The length of each TT capacitor is now $l_{eff} = (4{,}5\text{-}2)$ nm $= 2.5$ nm, since 2 nm are embedded in part of already calculated capacitor $C_0^{(1)}$

$$C_0^{(2)} = \frac{26 \times 6.28 \times 8.85 \times 10^{-12} \times 80 \times 2.5 \times 10^{-9}}{\ln(1 + (0.67/2.5))} = 1 \times 10^{-15} \text{ F} \tag{5}$$

Two above capacities are being connected in parallel, so the total maximal capacity of the ER is now estimated to be

$$C_0 = C_0^{(1)} + C_0^{(2)} = 1.8 \times 10^{-15} \text{ F} \tag{6}$$

It was already mentioned that the increase of negative voltage should increase the concentration of positive counter-ions in IC. These ions additionally condense on the surface of a MT and on its TTs. This brings about β-TTs to shrink diminishing their effective length $l_{eff} = 4.5$ nm, and thus the capacity $C_0^{(2)}$. It is reasonable to assume that this change of capacity is linear with respect to the applied voltage. This circumstance is of fundamental importance for establishing of an adequate model of MTs as nonlinear transmission lines for ionic currents. It will be elaborated in next Section in details.

2.2. The Effective Inductance of an ER in MT

The straightforward calculation performed in Ref. [4] revealed that the order of magnitude of the inductance of an ER in MT is of the order of $L \sim 10^{-15}$ H. This is very small value regarding pertaining reactive resistance. For example, if the frequency ω is of the order of MHz we have $\omega L \sim 10^{-9}$ Ω while capacitive impedance amounts $1/(\omega C) \sim 10^{9}$ Ω. Similar discrepancy holds for the energies of corresponding fields

$$\frac{1}{2} L i^2 \ll \frac{1}{2} C_0 v^2 \tag{7}$$

since i is of the order of nA and v of the order of several mV. Thus, the role of inductance in this model could be safely ignored. This circumstance removes the discrepancy between estimated wave velocity obtained for ionic current along actin filament[14] and the experimental evidences.

2.3. The Ohmic Resistance of an ER in MT

We here safely rely on recently published experimental findings, regarding electro-orientation method, performed by MTs *in vitro*.[15] This assay provided the value of MT conductivity as follows:

$$\sigma = (0.15 \pm 0.01) \frac{S}{m} \tag{8}$$

If we now take that the resistivity within an IC around a MT (with the thickness λ) is roughly homogeneous, the resistance of the ER with length $l = 8 \times 10^{-9}$, and the area $A = 2\ \pi R \lambda$, see Figures 4(a, c), is estimated to be of the order of:

$$R = \frac{1}{\sigma} \frac{l}{2\pi R \lambda} = \frac{8 \times 10^{-9}}{0.15 \times 2\pi \times 12.5 \times 10^{-9} \times 2 \times 10^{-9}} \ \Omega = 0.34 \times 10^{9} \ \Omega \tag{9}$$

2.4. The Nano-Pores in MT

The structural design of the MT is remarkable in terms of its biological functions. By cryoelectron microscopy, the group led by Nogales,[16] performed an assay which clearly revealed that between tubulin dimers within MT wall the conical NPs of about 1.7 nm in diameter exist, Figure 5. These NPs are characterized by the presence of the α-helix, H6, which can move down in MT structure increasing the effective size of the holes enhancing the diffusion of small ligands and ions into the MT lumen and vice versa. It could be expected that this movement may be controlled by physiological conditions.

We believe that NPs in MT are not just tubes that allow diffusion across it, but more sophisticated molecular machines able to respond on the changes in their environment and undergo precisely timed conformational change in order to be selective and to tune electric currents and signals confined within considered IC.

For comparison, it is well known that some ionic channels in cell membrane are being gated by ATP hydrolysis.[17] We could speculate that in the case of NPs in MTs the hydrolysis of GTP ligand binding process could cause the mentioned movement of H6, thus gating them. Such closed NPs are being open after an activation signal (in this case electrical) passes by. We here pay attention

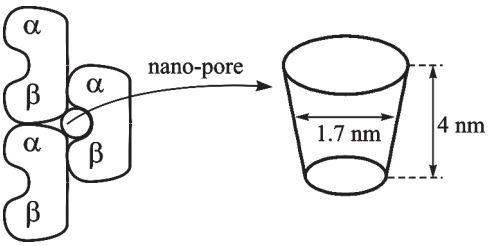

Fig. 5. The sketch of a NP with approximates shape and dimensions, the conical shape follows from MT geometry.

RESEARCH ARTICLE

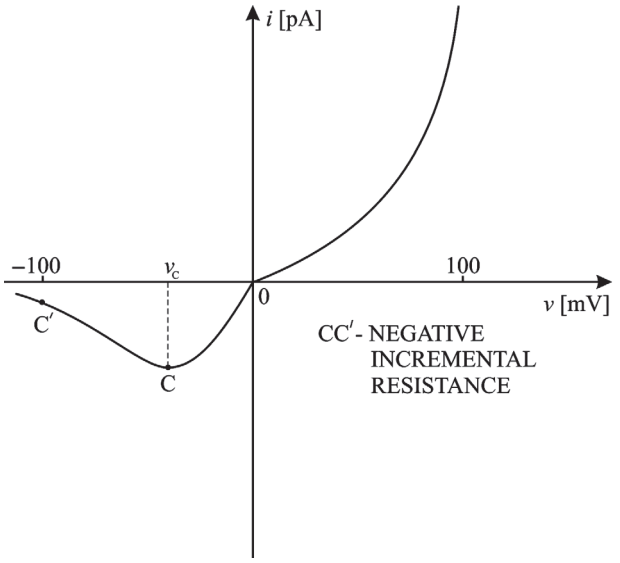

Fig. 6. The qualitative shape of current–voltage characteristics for NPs in the context of Eisenberg's group's work.[9,10] The segment CC′ shows the negative incremental resistance.

on the possible role of calcium ions which are good candidates for being injected from endoplasmic reticulum, and thus transported along MTs.

The group lead by Eisenberg[9,10] examined an artificial single asymmetric conical ionic NP-system whose rectifying properties for ionic current are changed dramatically by addition of a small concentration of calcium ions. They suggest that binding and unbinding of calcium ions to the pore walls produces pumping of potassium ions, by a flashing-rachet mechanism. This simplified case could suggest that we envisage NPs in MT as possible candidates for this kind of calcium-induced voltage gating. Nevertheless NPs in MTs are much more complex because the potential across the NP is a dynamic variable, hence the conductive properties of the pore must vary accordingly.

We could start this segment by the fact that voltage–current functions for mentioned artificial NPs with calcium-gating exhibit negative incremental resistance for a specific domain of sufficient negative voltage across NPs, Figure 6, section C–C′.[9,10] The threshold voltage v_c depends on calcium concentration and on overall characteristics of NPs. But we will later include the effects of nonlinear dynamical variations of NPs conductivity within MT.

3. THE MODEL OF MT AS A NONLINEAR TRANSMISSION LINE

On the basis of above estimations for the resistive components of the ER of a MT we are now in the position to establish the corresponding model. We consider a long transmission line (or ladder networks) composed of lumped sections equal to ERs. A typical section scheme is shown in Figure 7.

The longitudinal current is represented by the series of negligible inductance L_n and ohmic resistance R_n for one ER, as being estimated in previous section. The nonlinear capacity charged with Q_n is in parallel with total conductance of all NPs, G_n contained in an ER of the length $l = 8$ nm. This is because we consider the bulk cytosol and MT lumen as grounded. Applying Kirchoff's low to ladder of ERs, envisaged to represent coupled electrical circuits, we have

$$i_n - i_{n+1} = \frac{\partial Q_n}{\partial t} + G_n v_n \tag{10}$$

$$v_{n-1} - v_n = R_n i_n \tag{11}$$

We already stressed that the ER's capacitance C_0 must change with an increasing concentration of counter-ions due to the shrinking of flexible β-TTs. This implies that the charge on this capacitor diminishes with increased voltage in a nonlinear way as follows:

$$Q_n = C_0(1 - bv_n)v_n \tag{12}$$

where b is expected to be small enough ($bv_n \ll 1$) since the change of the area of a β-TT is small compared with total

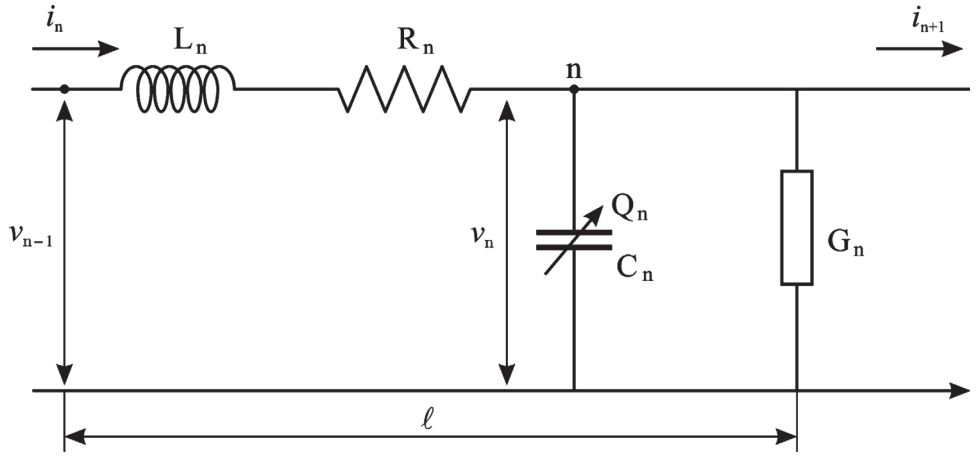

Fig. 7. An effective circuit diagram for the n-th ER with characteristic elements for Kirchoff's laws.

outer surface of the corresponding tubulin dimmer plus surface of α-TT. Now, we pay attention on the role of NPs in the context of negative incremental resistance (conductance) discovered by Eisenberg's group.[9, 10] We upgraded this idea by choosing the conductance of NPs to have the form dependent of voltage

$$G_n = -G_0\left(1-\beta\frac{dv_n}{dt}\right) \tag{13}$$

thus bringing an additional nonlinearity of system.

Replacing (12) and (13) in Eq. (10), one gets

$$i_n - i_{n+1} = -G_0 v_n + C_0\frac{\partial v_n}{\partial t} + \beta G_0 v_n\frac{\partial v_n}{\partial t} - 2bC_0 v_n\frac{\partial v_n}{\partial t} \tag{14}$$

$$v_{n-1} - v_n = R_n i_n \tag{15}$$

We now introduce the characteristic impedance of our system

$$Z = \frac{1}{C_0\omega} \tag{16}$$

and establish new function $u(x, t)$, unifying voltage and current as follows

$$u_n = Z^{1/2} i_n = Z^{-1/2} v_n \tag{17}$$

Bearing in mind that voltage v_n and current i_n change gradually from ER_n to its neighbors, we can safely expand u_n in a continuum approximation using a Taylor serie in terms of a small spatial parameter l (the length of a dimmer):

$$u_{n\pm1} = u \pm l\left(\frac{\partial u}{\partial x}\right) + \frac{l^2}{2!}\left(\frac{\partial^2 u}{\partial x^2}\right) \pm \frac{l^3}{3!}\left(\frac{\partial^3 u}{\partial x^3}\right) + \frac{l^4}{4!}\left(\frac{\partial^4 u}{\partial x^4}\right) \pm \ldots \tag{18}$$

By using Eqs. (16–18), system of Eqs. (14) and (15) now reads

$$\frac{\partial u}{\partial x} + \frac{l}{2}\frac{\partial^2 u}{\partial x^2} + \frac{l^2}{6}\frac{\partial^3 u}{\partial x^3} + \frac{l^3}{24}\frac{\partial^4 u}{\partial x^4} + \frac{l^4}{120}\frac{\partial^5 u}{\partial x^5} - G_0 Z u + \frac{ZC_0}{l}\frac{\partial u}{\partial t} + \frac{\beta Z^{3/2} G_0}{l} u\frac{\partial u}{\partial t} - \frac{2bZ^{3/2}C_0}{l} u\frac{\partial u}{\partial t} = 0 \tag{19}$$

$$\frac{\partial u}{\partial x} - \frac{l}{2}\frac{\partial^2 u}{\partial x^2} + \frac{l^2}{6}\frac{\partial^3 u}{\partial x^3} - \frac{l^3}{24}\frac{\partial^4 u}{\partial x^4} + \frac{l^4}{120}\frac{\partial^5 u}{\partial x^5} - \frac{RZ^{-1}}{l} = 0$$

Adding last two equations and neglecting terms beyond the order of l^5, we get

$$2\frac{\partial u}{\partial x} + \frac{l^2}{3}\frac{\partial^3 u}{\partial x^3} + \frac{1}{l}\left(RZ^{-1} - G_0 Z\right)u + \frac{ZC_0}{l}\frac{\partial u}{\partial t} + \left(\frac{\beta Z^{3/2} G_0}{l} - \frac{2bZ^{3/2}C_0}{l}\right)u\frac{\partial u}{\partial t} = 0 \tag{20}$$

We proceed by imposing the condition that third term in above equation should be zero

$$(RZ^{-1} - G_0 Z) = 0 \tag{21}$$

This condition enables that the ohmic loss could be balanced by fresh ions injected from NPs since these act as ionic pumps in suitable voltage regime.

It is now the important step to go over to dimensionless variables. In that respect, we introduce the characteristic scales of time and length. The characteristic time of charging ER-capacitor C_0 is $\tau = RC_0$. Taking the values of Eqs. (6) and (9), we have

$$\tau = 0.34\times10^{9}\times1.8\times10^{-15}\ \text{s} = 0.6\times10^{-6}\ \text{s} \tag{22}$$

The characteristic velocity of spreading the ionic wave is $v_0 = l/\tau$, which yields

$$v_0 = \frac{8\times10^{-9}}{0.6\times10^{-6}} = 13.3\ \frac{\text{mm}}{\text{s}} \tag{23}$$

Now we will use the standard travelling-wave form for unified function $u(x, t)$:

$$u(x,t) = u\left(\frac{x}{l} - v\frac{t}{l}\right) = u\left(\frac{x}{l} - \frac{v}{v_0}v_0\frac{t}{l}\right) = u\left(\frac{x}{l} - s\frac{t}{\tau}\right);\quad s = \frac{v}{v_0} \tag{24}$$

Introducing joined space-time dimensionless variable

$$\xi = \frac{x}{l} - s\frac{t}{\tau} \tag{25}$$

we have

$$\frac{\partial u}{\partial x} = \frac{1}{l}\frac{du}{d\xi};\quad \frac{\partial^3 u}{\partial x^3} = \frac{1}{l^3}\frac{d^3 u}{d\xi^3};\quad \frac{\partial u}{\partial t} = -\frac{s}{\tau}\frac{du}{d\xi} \tag{26}$$

It brings Eq. (20) into the form of ordinary differential equation, as follows

$$\frac{d^3 u}{d\xi^3} - 3\left(\frac{ZC_0 s}{\tau} - 2\right)\frac{du}{d\xi} + 3\frac{(2Z^{3/2}bC_0 - Z^{3/2}\beta G_0)s}{\tau} u\frac{du}{d\xi} = 0 \tag{27}$$

If we go back to the definition $u = Z^{1/2} i$, and then introduce the dimensionless current $W = i/i_0$, with i_0 being the peak value, we have

$$u = Z^{1/2} i_0 W = Z^{1/2} i \tag{28}$$

Inserting Eq. (28) into (27) yields

$$\frac{d^3 W}{d\xi^3} - 3\left(\frac{ZC_0 s}{\tau} - 2\right)\frac{dW}{d\xi} + 3\frac{i_0 s}{\tau}(2Z^2 bC_0 - Z^2\beta G_0)W\frac{dW}{d\xi} = 0 \tag{29}$$

Introducing the abbreviations

$$A = 3\left(\frac{ZC_0 s}{\tau} - 2\right); \quad B = 3\frac{i_0 s}{\tau} Z^2 (2bC_0 - \beta G_0) \quad (30)$$

we have

$$\frac{d^3W}{d\xi^3} - A\frac{dW}{d\xi} + BW\frac{dW}{d\xi} = 0 \quad (31)$$

After two successive integrations with the appropriate boundary conditions as follows

$$W_\infty = \left(\frac{dW}{d\xi}\right)_\infty = 0$$

one gets

$$\frac{dW}{d\xi} = \left(\frac{B}{3}\right)^{1/2} (DW^2 - 2W^3)^{1/2}; \quad D = \frac{3A}{B} \quad (32)$$

By introducing the new variable y

$$W = \frac{1}{2} D \cos h^2(y) \quad (33)$$

we finally obtain

$$W = \left[\frac{3(s\sigma - 2)}{s\sigma i_0 Z(2b - \beta(G_0/C_0))}\right] \times \sec h^2\left\{\frac{1}{2}\left[\frac{3}{2}(s\sigma - 2)\right]^{1/2}\left(\frac{x}{l} - s\frac{t}{\tau}\right)\right\} \quad (34)$$

with

$$\sigma = \frac{ZC_0}{T} \quad (35)$$

Let us estimate the dimensionless parameter σ. Starting from $Z = 1/C_0\omega$ we get $\sigma = 1/\tau\omega$. If we choose the moderate frequency of range $\omega = 10^4$ s^{-1}, which is based on the fact that the characteristic oscillations of ionic currents in Ref. [13] are of the order of kHz. Combining it with Eq. (22), it readily follows

$$\sigma = \frac{1}{6 \times 10^{-7} \times 10^4} = 1.67 \times 10^2 \quad (36a)$$

Accordingly the pertinent impedance reads

$$Z = \frac{1}{C_0\omega} = 5.56 \times 10^{10}\ \Omega \quad (36b)$$

Taking from the definition $i = i_0 W$, the IC current now has the form:

$$i(x,t) = \left[\frac{3(s\sigma - 2)}{s\sigma Z(2b - \beta(G_0/C_0))}\right] \sec h^2\left\{\frac{1}{2}\left[\frac{3}{2}(s\sigma - 2)\right]^{1/2}\left(\frac{x}{l} - s\frac{t}{\tau}\right)\right\} \quad (37)$$

This solution we will call ionic cloud soliton (ICS). It is apparent that down-limit of it velocity follows from the necessary condition

$$s\sigma - 2 > 0 \quad (38)$$

yielding

$$s \geq 1.2 \times 10^{-2} \quad (39)$$

Relying on Eq. (23) we now have the inequality for the speed of ICS

$$v > 0.16\ \frac{\text{mm}}{\text{s}} \quad (40)$$

Interestingly that the upper limit of ICS speed also exists on the basis of condition that its minimal width d can not be smaller of the length of one ER:

$$d = \frac{l}{1/2[(3/2)(s\sigma - 2)]^{1/2}} \geq l; \quad s\sigma \leq \frac{14}{3} \quad (41)$$

It gives

$$s \leq 2.8 \times 10^{-2} \text{ or } v \leq 0.34\ \frac{\text{mm}}{\text{s}} \quad (42)$$

Thus we get a pretty narrow window of possible solitonic speeds

$$(0.16 \leq v \leq 0.34)\ \frac{\text{mm}}{\text{s}} \quad (43)$$

In the other hand, using the balance condition, Eq. (21) we may estimate the negative conductance of NPs contained in an ER:

$$G_0 = \frac{R}{Z^2} = \frac{3.4 \times 10^8 \Omega}{5.6^2 \times 10^{20} \Omega^2} = 1{,}1 \times 10^{-13}\ \text{Si} \quad (44)$$

The order of magnitude of corresponding current is

$$i_{\text{NP}}^{(13)} = vG_0 = 0.1\ \text{V} \times 1{,}1 \times 10^{-13}\ \text{Si} = 1,1 \times 10^{-14}\ \text{A} \quad (45)$$

If the conductance nonlinearity parameter (βG_0) is much smaller than capacitance one, (bC_0) the ICS has very small amplitude of the order of 0.3 pA. But in the case where the conductance nonlinearity is getting competitive with capacitance nonlinearity, the ICS amplitude increases accordingly.

Thus, if we take $\sigma s = 2.5$, and assuming small margin of nonlinearities as follows

$$2b - \beta\frac{G_0}{C_0} = 0.1$$

which with $Z = 5.56 \times 10^{10}\ \Omega$, Eq. (37), yields:

$$i_0 = 27\ \text{pA} \quad (46)$$

If we compare it with experimental evidence from,[13] where the collected currents were in the range (2–6) nA, we could infer that dozens of ICS constituting the train-like pulses are involved in measured currents along MT.

Interestingly, the nonlinearities in NP conductance and TTs capacity have the opposite signs. This is the consequence of the fact that pumping of positive ions (potassium) by NPs from MT lumen causes diminishing of TTs capacity, and vice versa. The opposite signs of two nonlinearities lead to increase of amplitude of ICS, but do not affect its width and speed. We stress here that this bell-shaped ICS qualitatively differs from the localized wave obtain in Ref. [4] which was anti-kink-like.

We have shown a couple of numerical illustrations of ICS for different values of $s\sigma$ as represented in Figure 8.

We here emphasize that ICSs of our model exhibit the typical properties of KdV solitons in fluid dynamics. Their velocities are bellow the characteristic velocity v_o and increasing the velocity leads to increase of their amplitude and decrease of corresponding width (higher localisation).

Eventually, we could estimate the charge carried by one ICS with $s\sigma = 3$. Starting from $Q_n = C_0(1 - bv_n)v_n$ and using continuum approximation, the total charge is

$$Q = \frac{C_0}{l}\int_{-\infty}^{+\infty}(v - bv^2)\,dx; \quad v(x,t) = Z \cdot i(x,t) \tag{47}$$

or explicitly:

$$Q = \frac{C_0}{l}\left[i_o Z\right]\int_{-\infty}^{+\infty}\operatorname{sec h}^2\left\{\frac{1}{2}\left[\frac{3}{2}\times 1\right]^{1/2}\left(\frac{x}{l} - s\frac{t}{\tau}\right)\right\}dx$$
$$-\beta\frac{C_0}{l}[i_0 Z]^2\int_{-\infty}^{+\infty}\operatorname{sec h}^4\left\{\frac{1}{2}\left[\frac{3}{2}\times 1\right]^{1/2}\left(\frac{x}{l} - s\frac{t}{\tau}\right)\right\}dx$$

The second addend could be safely ignored, as very small. Using Eq. (47) with already known parameters C_0, Z and $i_0 = 27$ pA, yields

$$Q = 2.7\times 10^{-15}\ \text{C} = 1.7\times 10^4\ \text{e} \tag{48}$$

One could also assess the energy carried by an ICS. The basic assumption is that the energy loss due to the ohmic resistance is being compensated through fresh supply of ions by NPs. Under such circumstances it is clear that the energy contained in ER capacitors should be preserved. This energy amounts:

$$E = \frac{Q^2}{2C_0} = \frac{(2.7\times 10^{-15}\ \text{C})^2}{2\times 1.8\times 10^{-15}\ \text{F}}$$
$$= 2\times 10^{-15}\ \text{J} = 1.7\times 10^4\ \text{eV} \tag{49}$$

Taking the charge of $Q = 1.7\times 10^4$ e, Eq. (3.39), to be attributed to monovalent ions, the energy per single ion involved in ICS is of the order of 0.8 eV which is one thirty times greater of thermal energy (25 meV).

4. THE INFLUNCE OF VISCOUS DISSIPATION AND INTRINSIC ELECTRIC FIELDS ON THE DYNAMICS OF ICSs ALONG MTs

In the absence of dissipation the ICS, Eq. (46), is expected to move at a constant speed s. But, since ICS behaves like

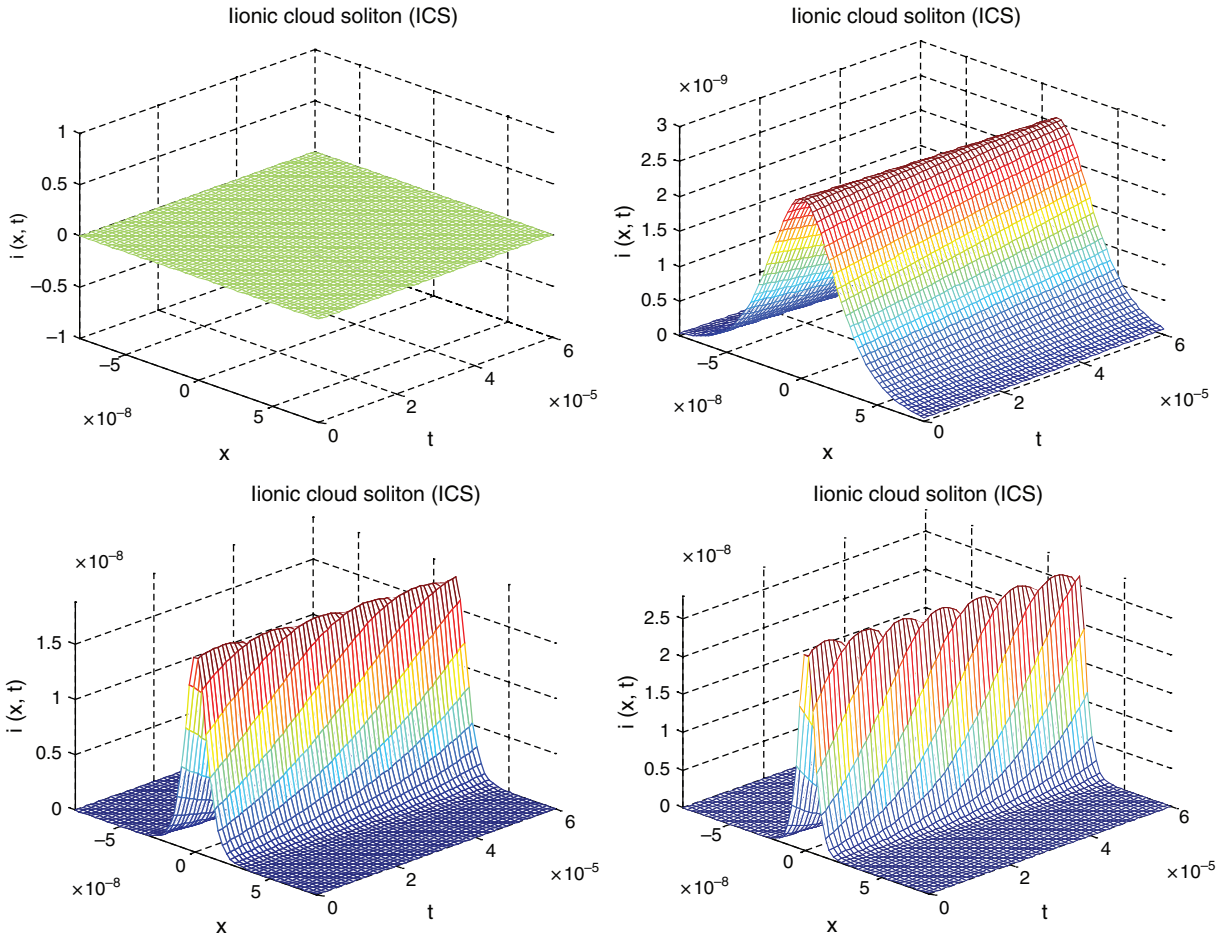

Fig. 8. Numerical solutions: (a) for $s\sigma = 2$ (the smearing limit), (b) for $s\sigma = 2.1$, (c) for $s\sigma = 3$ and (d) for $s\sigma = 4$.

RESEARCH ARTICLE

a "particle" in a viscous fluid, it is evident that the role of viscous cytosol is to decrease its speed.

The rate of deceleration could be calculated on the basis of Energy method.[18, 19] This rate appears to follow exponential decay tending to the down-limit ($s\sigma = 2$), Eq. (38), when ICS is being totally smeared out.

In the other hand, since ICS is being subjected under the action of intrinsic electrical field of MT[20, 21] it should be accelerated.

The most interesting case is when these two opposite tendencies are mutually balanced. The viscous damping is proportional to the speed of an ICS:

$$F_{\text{vis}} = -kv \tag{50}$$

where k depends on dynamical viscosity of cytosol and on the geometry of ICS, while the force of electric field simply reads

$$F_{\text{if}} = Q \cdot E_i \tag{51}$$

with E_i being the strength of intrinsic electrical field along MT.

Equations (50) and (51) we can calculate the value of parameter k on the basis of estimated $E_i = 10^4$ V,[21] and taking $v = 0.2$ mm/s, and Q from Eq. (48), we get

$$k = \frac{Q \cdot E_i}{v} = \frac{2.7 \times 10^{-15} \times 10^4}{0.2 \times 10^{-3}} = 1.35 \times 10^{-7} \ \frac{\text{kg}}{\text{s}} \tag{52}$$

Obviously the strength of intrinsic electric field could be an important mechanism for tuning dynamics of ICS.

5. CONCLUSION AND DISCUSSION

We here farther improved the former model[3, 4] for ionic currents propagating in narrow layer along MTs. This model is established in terms of polyelectrolyte concept applied to the molecular structure and geometry of MT, and taking into account its interaction with solvent ions. As the consequence, the MT cylinder with flexible TTs, surrounded by counter-ions from cytosol, is considered as an electrical transmission line, with R, C and G elements estimated on the basis of approximate MT geometry and other experimental evidences available. The essentially important nonlinearity of model pertains to its capacitance arising from structure and dynamics of β-TTs and from dynamic conductance of NPs.

We here paid the particular attention to the possible role of NPs acting as ionic pumps thus creating the negative incremental resistance in the considered circuit.

As a result, the nonlinear second order differential equation for ionic current along MT was evaluated. The travelling-wave solution of Eq. (48) is localized ICS which exhibits the features of celebrated Korteveg de Wries soliton from fluid dynamics. It is important to emphasize the qualitative difference of this bell-shaped ICS compared with anti-kink solution obtained in former approach.[4] It appears that the role of NPs exerts some kind of self-focusing effect on IC increasing its amplitude.

Interestingly, this ICSs have pretty narrow window of possible velocities with the order of magnitude being a fraction of (mm/s), based on the assessed capacity and ohmic resistance of an ER of such transmission line.

We estimated the order of magnitude of pertaining current along a single MT, together with the charge of ICS and its energy. These parameters have pretty reasonable values, being comparable with still scarce experimental data.

Let us especially pay attention on the interesting experimental assay performed by the group led by Tuszynski.[13] The measured values for the ionic current along the single MT were in the range (2–6) nA. Moreover they stated that the electrical amplification by MTs is equivalent to their ability to act as the bimolecular living transistors. In that respect the NP current of pumped ions, Eq. (45), in our model is expected to play the control role as well as the base current does play in bipolar transistor.

It is worth to mention the experimental results regarding intracellular calcium dynamics.[22] Calcium ions released from endoplasmic reticulum could be candidate for propagation along MT in the context of present model. The calcium puffs launched from above compartment could have enough energy (proper velocity) to form ICS. This localized propagation of ions is being controllable by cellular electric fields and goes faster than the pure diffusion through cytosol. Experimental speed of diffusive calcium waves, according to Ref. [22], is of the order of 12 (μm/s), which is one order of magnitude bellow the ICS window, Eq. (43).

We finally considered biophysically realistic circumstances where the damping effects are being balanced by energy supply provided by existing cell's intrinsic electrical fields.

Our results could encourage experimentalists to conduct more subtle assays in an attempt to ellucidate this important aspect of cellular activities.

Acknowledgment: This research was supported by funds from Serbian Ministry of Science, Grants 1411018A, TP 11023 and TP 11006.

References

1. M. Satarić, L. J. B. Petković, I. Lončarević, and J. A. Tusyznski, *Biophys* 52, 113 (**2008**).
2. M. Satarić, L. J. B. Petrović, and I. Lončarević, *JJMPB* 21, 5387 (**2007**).
3. M. V. Satarić, D. Ilic, and N. Ralecic, *Chin. Phys. Lett.* 26, 073101 (**2009**).
4. M. V. Satarić, D. I. Ilić, N. Ralević, and J. A. Tuszynski, *Eur. Biophys. J.* 38, 637 (**2009**).
5. J. A. Tusyznski, J. A. Brown, E. Crowford, E. J. Carpenter, M. L. A. Nip, J. M. Dixon, and M. V. Satarić, *Math. Comput. Model* 41, 1055 (**2005**).
6. T. Polard and J. Cooper, *Ann. Rev. Biochem.* 55, 987 (**1986**).

RESEARCH ARTICLE

7. J. A. Tuszynski, S. Portet, J. M. Dixon, C. Luxford, and H. F. Cantiello, *Biophys. J.* 86, 1890 **(2004)**.
8. M. V. Satarić, N. Bednar, B. M. Satarić, and G. Stojanović, *IJMPB* 30, 1 **(2009)**.
9. Z. S. Siwy, M. R. Powell, A. Petrov, E. Kalman, C. Trantmann, and R. S. Eisenberg, *Nano. Lett.* 6, 1729 **(2006)**.
10. Z. S. Siwy, M. R. Powell, E. Kalman, R. D. Astumian, and R. S. Eisenberg, *Nano. Lett.* 6, 473 **(2006)**.
11. E. C. Lin and H. F. Cantiello, *Biophys. J.* 65, 1371 **(1993)**.
12. K. E. Lonngreen, In Solitons in Action, Academic Press, New York **(1978)**.
13. A. Priel, A. J. Ramos, J. A. Tuszynski, and H. F. Contiello, *Biophys. J.* 90, 1 **(2006)**.
14. J. A. Tusznyski, S. Portet, J. M. Dixon, C. Luxford, and F. H. Contiello, *Biophys. J.* 86, 1890 **(2004)**.
15. I. Minoura and E. Muto, *Biophys. J.* 90, 3739 **(2006)**.
16. H. Li, D. J. De Rosier, W. V. Nickolson, E. Nogales, and K. H. Downing, *Structure* 10, 1317 **(2002)**.
17. J. G. Orlandi and J. M. Sancho, *Eur. Phys. J. E* DOI 10.1140/epje/i2009-10483-0 **(2009)**.
18. A. C. Scott, F. Y. Chu, and D. W. Mac Laughlin, *Proc. IEEE* 61, 1443 **(1973)**.
19. L. V. Yakushevich and L. A. Krasnobaeva, *Biophysics* 52, 237 **(2007)**.
20. M. V. Sataric, J. A. Tuszynski, and R. B. Zakula, *Phys. Rev. E* 48, 589 **(1993)**.
21. M. V. Sataric and J. A. Tuszynski, *Phys. Rev. E* 67, 011901 **(2003)**.
22. K. Wnag, W. Jan Rappel, and H. Levine, *Phys. Biol.* 1, 27 **(2004)**.

Received: 3 January 2010. Accepted: 3 March 2010.

RESEARCH ARTICLE